Sea Modeling by Microwave Altimetry

STEFANO PIERINI
Dipartimento di Fisica (INFM), Università dell'Aquila, Italy.

Key words: Altimeter, geostrophic currents, ocean modelling

Abstract: In this note the applications of altimeter data to the monitoring of the sea surface height and, in particular, to the evaluation of large-scale oceanic currents are reviewed. The general problem of the altimeter measurement, with a special reference to the TOPEX/POSEIDON mission, is discussed. The decomposition of the sea surface height anomaly into its various components (tides, inverted barometer, steric height, height associated to geostrophic currents) is then considered. For each component a brief description of the physics of the associated phenomenon is given, along with references to the related recent scientific literature. A special emphasis is put on the determination of oceanic geostrophic currents. Therefore, the methods used to eliminate the components of the sea surface height anomaly not related to geostrophy are discussed. The derivation of near-surface currents and of depth-dependent currents with the aid of hydrographic data is considered in some detail. Finally, oceanic wind-driven models, in particular the time-dependent Sverdrup balance, are discussed in connection with altimeter data.

1. INTRODUCTION

The altimetry is a spaceborne microwave radar that is able to measure with an extremely high accuracy the distance between the satellite carrying the instrument and the sea surface. This has very important implications concerning different aspects of the earth sciences, such as the accurate determination of the earth shape (including the ocean bathymetry), the analysis of the oceanic tides and the monitoring of relevant aspects of the ocean circulation. In Section 2 the general problem of altimeter measurements, with particular attention to the TOPEX/POSEIDON mission

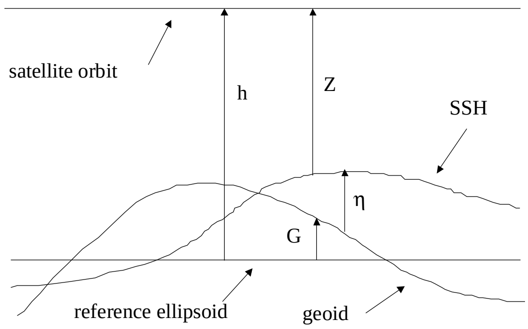

Figure 1. Definition of the parameters h, G, Z and η.

and to the current inadequacy of altimeter data to study mean currents, will be reviewed. In this note we will put the stress on oceanographic implications, namely on the determination from altimeter data of time-varying geostrophic currents associated to the dynamically active part of the sea-surface height (SSH) anomaly. From our point of view we will therefore consider the remaining part of the altimeter signal as a “noise” to be filtered out. Section 3 is devoted to the analysis of these effects and to the methods that can be adopted in order to remove them. In section 4 the computation of near-surface geostrophic currents from the dynamically active SSH anomaly, and of the current vertical shear with the aid of hydrographic data are discussed. In the same section the observation of Rossby waves with the altimeter is also briefly considered. Finally, in Section 5 oceanic wind-driven models, with particular emphasis on the time-dependent Sverdrup balance, are considered in connection with altimeter data.

2. ALTIMETER DATA AND THE VARIABILITY OF THE SSH

The general problem posed by the altimeter measurements can be summarized as follows (e.g., Robinson, 1994). Let us define a “reference ellipsoid” as the one that approximates the shape of the earth surface without considering small scale anisotropies in the distribution of mass. This ellipsoid has R_{min}=6357 km and R_{max}=6378 km, where R_{min} is the polar radius and R_{max} is the equatorial radius. The satellite orbit (*h*), and the “geoid” (*G*) are referred to this reference surface. The geoid is the geopotential surface that would coincide with the sea surface if the sea were in equilibrium, and presents small scale departures from the reference ellipsoid (ranging from -104 m to +64 m) because anomalies in the distribution of mass are present. It is therefore natural to refer the sea-surface height (η) to the geoid, and finally let us denote as Z the altimeter data measured by the radar (Fig. 1).

The oceanographically interesting quantity η, referred to a given point of the sea surface, will therefore be given by:

$$\eta(t) = h - G - Z(t) \ . \tag{1}$$

Let us now discuss briefly the errors associated to each quantity. Starting from the Skylab mission (1973-1974), passing through GEOS 3 (1975-1978), Seasat (1978), Geosat (1985-1989), ERS 1/2 (1991-2000/1995) and arriving to the joint United States/French mission TOPEX/POSEIDON (from now on denoted as T/P), the accuracy in the determination of each of these variables has greatly improved. For the T/P data, which are the ones we will be mainly concerned with in this note, both the satellite orbit determination h and the altimeter measurement Z are affected by an error of only 3-5 cm, which is astonishingly small if compared to the orbital altitude of O(1000 km). One should bear in mind that to achieve such a high degree of accuracy for h and Z it is not only necessary to have a state-of-the-art radar, but it is also fundamental to introduce appropriate corrections for atmospheric transmission and surface roughness errors and, as far as h is concerned, it is necessary to rely on a satisfactory satellite orbital model which, fortunately, does not depend heavily on the small scale variations of the geoid.

Before proceeding to the analysis of the errors, let us spend few words on the T/P mission. The satellite was launched in August 1992 and was expected to operate through September, 1998, although the satellite was operational for a longer time (see the special section of the *Journal of Geophysical Research*, 99 (C12), 24,369-25,062, 1994, devoted to “TOPEX/POSEIDON: Geophysical Evaluation” for general aspects of the mission, the gravity model, the orbit determination and their accuracy). The orbital altitude was chosen relatively high (1336 km) in order to reduce atmospheric drag and gravity forces acting on the satellite, and therefore maximizing the accuracy of orbit determination. The repeat period (9.916 days), the inclination (66 degrees), and the cross-track separation (316 km at the equator, 240 km at 40°) insure a good compromise for the temporal and spatial resolutions, and avoid undesirable aliasing problems for the tidal constituents (Fu et al., 1994).

Now, if the geoid G were affected by an error comparable or smaller than that of h and Z, then the altimeter mapping of a given sea region would provide the SSH within an error of 3-5 cm. In particular, as the repeat period of T/P is ~10 days, a large scale oceanic region would be covered in a time smaller than most oceanic variability, therefore the obtained η over that area could be seen as an "instantaneous" picture of the sea surface topography and (as we will see in sect. 4), indirectly, of geostrophic currents. However, the geoid is still affected by an error larger than 3-5 cm, ranging from more than 20 cm for relatively small spatial scales (the interesting ones for oceanographic applications) to 10 cm for scales larger than 2000 km, and this makes the determination of the instantaneous currents inaccurate. Let us consider, for instance, the JGM-3 Ohio State University (OSU91a) geoid model developed by the T/P project (Rapp et al., 1991; Nerem et al., 1994; Tapley et al., 1996). Stammer et al. (1996) computed the mean SSH averaged over a 2-year period from T/P data relative to this geoid model (in other words they took a long time average of (1), obtaining a given $<\eta>$). They then subtracted this "measured" mean SSH from the one ($<\eta>_{model}$) computed by the global Parallel Ocean Climate Model (POCM) of Semtner and Chervin (1992), which in this framework is considered as a reference "real" SSH. Major differences were indeed found primarily on relatively small scales, especially in oceanic trench systems where the geoid is known to be affected by large error estimates. It should be mentioned, however, that for particularly strong currents, such as for instance the Antarctic Circumpolar Current (ACC), the altimeter can provide information also on the mean flow (e.g., Park and Gambéroni, 1995). Recently a method to determine the mean SSH from altimeter data based on the knowledge of its temporal variability was proposed by Feron et al. (1998). It gives promising results for ocean areas with strong mesoscale variability, such as the western boundary currents and the ACC. However, in general, up to now geoid estimates appear to have proved inadequate to use altimetric data for improving the existing knowledge of the average large-scale oceanic circulation. A sufficiently accurate evaluation of the geoid for the computation of absolute currents is nevertheless expected in the near future.

On the other hand, in order to obtain interesting oceanographic information from *Z* one can take advantage of the fact that the satellite orbit is repeating, i.e. the ground tracks are repeatedly covered by the satellite, so that long time series are available. One can therefore define the SSH and altimeter measurement anomalies η' and Z', respectively, as follows:

$$\eta(t) = \langle\eta\rangle + \eta'(t), \quad Z(t) = \langle Z\rangle + Z'(t),$$

where <.> represents time averaging. Thus, by taking the average of (1) and subtracting the means one finally obtains:

$$\eta'(t) = -Z'(t). \tag{2}$$

This equation shows that the temporal anomaly of the SSH can be evaluated with the same accuracy of *h* and *Z* no matter how accurate is the geoid determination, the latter being eliminated by the averaging procedure along with the mean value of the SSH.

3. DECOMPOSITION OF THE SSH ANOMALY INTO ITS VARIOUS COMPONENTS

The dynamically active part (η'_D) of the SSH anomaly we are seeking for, i.e. the one related to geostrophic currents, is only one of the components into which the measured anomaly η' can be decomposed. One can write:

$$\eta' = \eta'_T + \eta'_P + \eta'_S + \eta'_D + \delta\eta' , \tag{3}$$

where η'_T is the SSH anomaly related to the ocean tides, η'_P is related to the isostatic response of the ocean surface to atmospheric pressure fluctuations, η'_S is the "steric" anomaly associated to the expansion or contraction of water due to heat exchange with the atmosphere and, finally, $\delta\eta'$ is the anomaly associated to errors and to all the other (mainly small scale) non-geostrophically balanced motions. Although (3) includes motions that have very different space and time scales (Wunsch and Stammer, 1995), nonlinear interactions can nonetheless be present. However, they are usually not very relevant, and here we assume that each term can be considered separately. In the remainder of this section the first three anomalies in (3) will be briefly considered. In the next two sections the dynamically active part of the signal will be discussed in more detail.

3.1 Tides

The knowledge of the ocean tides has greatly improved in the last two decades thanks both to the unprecedented accuracy and global coverage of the altimeter data, and to the implementation of numerical world tidal models. The tides are the only oceanic motions that can, in principle, be predicted provided the amplitudes and phases of all the consituents are known. The combination of altimeter data and models has, in fact, produced most accurate global maps of the tides which now have an accuracy of 2 cm in the deep ocean (Shum et al., 1997). The term η'_T can therefore be eliminated from (3), without modifying the accuracy of the balance, by means of state-of-the-art tidal models (e.g., Ma et al., 1994; Le Provost et al., 1994; Eanes and Bettadpur, 1995; Andersen at al., 1995). A brief discussion about the observation of tides with the altimeter is presented below.

In points along a repeat ground track altimeter data provide time series of η' that can be analysed by means of a spectral analysis, in a manner analogous to what is usually done with tide gauge data. Since the tidal frequencies are known, if the time series are long enough to resolve all the frequencies, the amplitudes and phases of the constituents can be determined. For altimeter data problems arise because the observed frequencies are not the effective tidal ones but they are alias frequencies because the signal is sampled at intervals longer than half the periods (for T/P we have seen that the cycle repeats every ~10 days while the main tidal components are semidiurnal and diurnal). To give an example, the T/P alias periods for M_2 (12.42 h), S_2 (12.00 h), K_1 (23.93 h), and O_1 (25.82 h) are: 62.11, 58.74, 173.19, 45.71 days, respectively (Schlax and Chelton, 1994). The time series must therefore be particularly long in order to resolve such low frequencies, but the long time coverage of T/P is sufficient to resolve the main constituents. For this kind of data the tidal analysis known as the "response method" is usually applied (e.g., Munk and Cartwright, 1966; Cartwright and Ray, 1990; Andersen, 1995). For the analysis of the global ocean tides in the deep ocean with T/P one can refer to Desai and Wahr (1995), Sanchez and Pavlis (1995), Andersen (1995), Andersen et al. (1995), Kantha (1995), Kantha et al. (1995), Matsumoto et al. (1995), Arnault and Le Provost (1997), Desai et al. (1997), and Tierney et al. (1998). Finally, it should be mentioned that, since in shallow coastal seas the tides are largely dependent on the bathymetry and the shape of the coasts, the resulting horizontal length scales can be very small, so that the altimeter cannot resolve the tides properly. Nevertheless reliable empirical estimates can be obtained from T/P by combining along-track and crossover observations (Andersen, 1999). The use of coastal ocean models can also prove very useful (Foreman et al., 1998).

3.2 Inverted Barometer

Let us suppose that in the open ocean a stationary horizontal atmospheric pressure gradient is present at the sea surface due to a perturbation p_a superimposed on the spatially averaged atmospheric pressure. The ocean is in equilibrium (absence of motion) only if no horizontal pressure gradient in the sea is present. Therefore the sea level must adjust in such a way that the corresponding pressure anomaly balances the one associated to the atmospheric pressure (e.g., Gill, 1982), i.e.:

$$\rho g \eta_P(x,y) = -p_a(x,y), \tag{4}$$

where ρ is the surface water density and g is the acceleration of gravity (for the sake of simplicity, rectangular coordinates are considered: x and y are horizontal coordinates on a tangent plane and z is the vertical coordinate). The SSH anomaly implied by (4) is that of an "inverted barometer", i.e. the local increase of the atmospheric pressure (e.g. of 1 mbar) is balanced by a depression of the sea surface (of 1 cm), so that at any depth in the sea no pressure difference is found (naturally, the sea surface topography is produced, during the transient, by the motion of water masses driven by the not yet balanced horizontal pressure gradient). Relation (4) is rigorously valid for a stationary pressure anomaly in an infinite ocean, but it applies also to realistic situations in which the pressure varies over periods longer than ~2 days (e.g., Ponte, 1992, 1993; Wunsch and Stammer, 1997). For these sufficiently long periods one can consider a quasi-isostatic balance given by (4) but where η and *p* are substituted by the fluctuations η' and *p'*:

$$\rho g \eta'_p(x,y,t) = -p'_a(x,y,t). \tag{5}$$

The T/P altimeter data have proved a powerful tool to test (4-5) and to study its departures (Fu and Pihos, 1994; Gaspar and Ponte, 1997; Ponte and Gaspar, 1999). On the other hand, the knowledge of the surface atmospheric pressure, provided for instance by the NCEP or ECMWF meteorological analysis, allows to remove, through (5), the term η'_P in (3) (e.g. Wunsch and Stammer, 1997; Stammer, 1997). It should be noticed that in a semi-enclosed sea such as the Mediterranean basin the assumption that the ocean be infinite is far from being satisfied, therefore more complex models than (5) should be adopted (e.g., Candela, 1991; Le Traon and Gauzelin, 1997).

For atmospheric pressure variations over time scales smaller than ~2 days the ocean does not respond isostatically, i.e. through (5), and even for periods longer than 2 days, oceanic rotational normal modes can be excited (e.g., Ponte, 1993, 1997; Pierini, 1996; Pierini et al, 2002) leading to time-dependent SSH signals. Therefore, it should be borne in mind that part of the oceanic response to the atmospheric pressure variability in terms of SSH is included in the last term $\delta\eta'$ in (3).

3.3 Steric height

The main cause of the variability of the SSH outside the tropics is the density variation of the water column (without change of mass) associated to the net surface heat flux. This is the so-called "steric height" change, denoted by η'_S in (3), and given by (Gill and Niiler, 1973):

$$\eta'_S = -\frac{1}{\rho_0}\int_{-H}^{0}\rho' dz \, , \qquad (6)$$

where ρ' is the density anomaly, ρ_0 is a reference mean density and *H* is the water depth, although the main changes take place in the thin surface mixed layer which is affected by atmospheric buoyancy fluxes (there is also an adiabatic steric effect associated with the vertical displacement of isotherms due to the wind, but we do not consider this effect here). The SSH steric anomaly has a pronounced seasonal variability and manifests itself over large spatial scales of O(1000 km). It increases with increasing latitude, and the T/P data have shown a somewhat surprising asymmetry in amplitude between the two hemispheres (Stammer, 1997). This signal is dynamically passive, because below the mixed layer no horizontal pressure gradient is associated to it, since no change in mass is produced. On the other hand, near the surface the SSH variations do cause pressure variations, but they are over such large scales that the corresponding horizontal pressure gradient force, and therefore the associated geostrophic currents, are negligible. The steric SSH anomaly is important *per se* because it allows to monitor the ocean heat storage (e.g., White and Tai, 1995; Chambers et al., 1998). However, how to get rid of this large anomaly when studying geostrophic currents? The most sophisticated method is the one adopted by Stammer (1997) and Vivier et al. (1999) who modelled the steric term (6) by using ECMWF net heat fluxes. The steric term is computed by Polito and Cornillon (1997) by using the NODC climatology and by Gilson et al. (1998) using a climatology consisting of XBT and XCTD profiles. One can also take advantage of the large-scale nature of the signal in order to filter it out by means of appropriate averaging procedures, as done by Isoguchi et al. (1997) and Witter and Gordon (1999).

4. GEOSTROPHIC CURRENTS AND ROSSBY WAVES

In this section we discuss the term η'_D in (3) associated with the geostrophic balance and for which, therefore, information on oceanic currents can be obtained. In order to do this we begin by reviewing some basic notions of dynamical oceanography. An oceanic current is said to be in geostrophic balance if the Coriolis force and the horizontal pressure gradient force balance out exactly. In this case the current velocity can be written in the *f*-plane as follows (e.g., Pedlosky, 1987; Gill, 1982; Pond and Pickard, 1983):

$$u = -\frac{\partial \psi}{\partial y}, v = \frac{\partial \psi}{\partial x}, \tag{7}$$

where the streamfunction ψ is given by:

$$\psi(x, y, z) = \frac{1}{\rho f} p(x, y, z),$$

(*p* is the sea pressure, ρ(x,y,z) is the water density and *f* is the Coriolis parameter). Equation (7) implies that geostrophic currents flow parallel to the isobars, and it is rigorously valid only if the acceleration vanishes, i.e. for rectilinear and stationary currents. However, for flows that are sufficiently large-scale, both in space and time (more precisely, for small Rossby number flows; see Pedlosky, 1987), equation (7) provides an excellent approximation, so that primed variables can be substituted in (7) (from now on the time dependence is understood to satisfy this requirement).

If currents near the sea surface (z=0) are considered, then *p'* can be expressed, through the hydrostatic relation, in terms of the SSH anomaly:

$$\psi'_{surface}(x, y, t) = \frac{g}{f} \eta'_D(x, y, t), \tag{8}$$

where the subscript *D* in η' indicates that we are now dealing with the dynamically active part of the SSH (see (3)). Equation (7) with (8) allows to derive the geostrophic surface current anomalies from the knowledge of the SSH anomaly as obtained from the altimeter, after subtracting other components not related to geostrophy, as discussed in sect. 3. This is the main scientific motivation on which the altimeter missions are based. Considering the error in the determination of η (sect. 2), large-scale altimeter-derived currents are, up to now, affected by an error of 3-5 cm/s (Strub et al., 1997). Examples of computation of upper ocean geostrophic currents from altimeter data (often performed by computing the along-track derivative of η'_D in order to avoid mapping errors, thus obtaining the cross-track velocity) are given by Kelly and Gille (1990), Yu et al. (1995), Larnicol et al. (1995), Snaith and Robinson (1996), Rapp et al. (1996), Strub et al. (1997), Iudicone et al. (1998), and Vivier and Provost (1999).

If surface geostrophic currents are interesting, even more important is the knowledge of the current as a function of depth or, at least, of depth-integrated currents, because they correspond to net heat oceanic transports that contribute substantially to the world climate. The altimeter cannot provide any direct information about this, but complementary in situ measurements can be used in conjunction with altimeter data in order to evaluate geostrophic currents at depth. We therefore pass to give a brief discussion on this topic. In a hypothetical homogeneous incompressible ocean a geostrophic current would be depth-independent, because no other source of horizontal pressure gradient but the one provided by the sea surface topography exists, therefore (7-8) would give the current at any depth. On the other hand, real oceans are stratified, a typical stratification consisting of a surface mixed layer followed by a region of sharp temperature variation (the thermocline), below which an almost constant-density water is present (but very large departures from this idealized picture can be present; see, for instance, Pickard and Emery, 1982). The presence of stratification is usually accompanied, for the mean flow, by a baroclinic compensation, which produces a geostrophic current that is small or even vanishes at great depth. In fact, the inclination of the isopycnic surfaces, produced by various causes, corresponds to a depth-dependent “relative” pressure field and, in turn, to a relative current field, which is the oceanic counterpart of the atmospheric “thermal wind” (e.g., Holton, 1979). This baroclinic current adds to the barotropic current given by (7-8), thus yielding a total depth-dependent geostrophic current, which reduces to (7-8) at the surface.

For the wind-driven circulation in large oceans, baroclinic compensation is the result of an adjustment process in which long baroclinic Rossby waves radiate from the eastern boundary (Anderson and Gill, 1975). At mid-latitudes the time needed to achieve this spin-up is of the order of a decade, therefore while the mean flow is compensated, the circulation induced by time-dependent winds is on the contrary mainly barotropic for periods less than O(1 year) (the barotropic spin-up is much faster, requiring only a few days to be effective). As a consequence, the current fluctuations measured by the altimeter for the same periods at mid-latitudes are expected to be representative not only of the subsurface dynamics but, to some degree, also of the entire water column. However, for lower latitudes the baroclinic spin-up time is sensibly smaller (the speed of Rossby waves increases rapidly toward the equator). Therefore near the tropics also the time-dependent ocean circulation yields a relevant baroclinic component. Apart from large oceans, in many other circumstances where coastal and topographic effects are important, relative currents can exist also for the time-dependent ocean circulation. Thus, the altimeter-derived SSH anomaly should, in general (but particularly at low latitudes), be complemented with in situ hydrographic measurements. Aspects related to this point will now be considered.

Hydrographic (i.e. temperature, salinity and pressure, and therefore density) measurements are performed by research vessels over large ocean areas and provide the vertical shear of the relative current through the thermal wind relationship, but no absolute current value. A classical problem of dynamical oceanography is the determination of the absolute current profile by prescribing a value of the current at some depth. This is often done by assuming a “level of no motion” in which the current vanishes (Pond and Pickard, 1983), although this “classical” method is affected by large uncertainties. Another more reliable method would be, in principle, that of using a “level of known motion” where geostrophic currents are known. This method is perfectly suitable for altimeter data because, as we have seen, the latter provide geostrophic surface currents, i.e. at $z=0$. The knowledege of the vertical derivative of the current given by the thermal wind (if the density structure is known) can therefore give the current also at $z<0$. Usually, the seasonal and longer term variability is analysed with this method. Examples of computation of geostrophic currents at depth from altimeter and hydrographic data are given by Han and Tang (1999), Buongiorno Nardelli et al. (1999), and Vivier and Provost (1999). An alternative way of computing currents below the surface from altimeter data is proposed by Williams and Pennington (1999) who, for a given background stratification in the North Atlantic, constrain a thermocline model by T/P altimetry, in so obtaining a relationship between SSH and the depth-integrated transport. Hydrographic data can also be used in an inverse way: for instance, in order to perform a quantitative test for an oceanic general circulation model, Stammer et al. (1996) use the SSH obtained by a global inversion of hydrographic and nutrient data along WOCE (World Ocean Circulation Experiment) sections and compare it with both model and altimeter-derived SSH.

Important dynamical features of the large scale oceanic variability that can be detected by the altimeter are Rossby waves (e.g., Pedlosky, 1987, 1996; Gill, 1982). They represent the messengers of energy in large scale (subinertial) atmosphere and ocean dynamics. In the oceans Rossby waves provide the dynamical mechanism for the adjustment to the large scale atmospheric forcing, and play a fundamental role in phenomena such as the westward intensification of boundary currents, the oceanic response to large scale fluctuating winds, boundary current radiation, etc.. Rossby waves are barotropic or baroclinic quasi-geostrophic current oscillations, and owe their existence to the conservation of potential vorticity of fluid columns in an ambient in which the planetary vorticity varies with latitude (the planetary β-effect), but a topographic counterpart also exists. Since Rossby waves are quasigeostrophic oscillations, (7-8) apply to them, therefore they can be revealed synoptically by the altimeter. This is a really revolutionary improvement in Rossby wave observation since, before, only local hydrographic, currentmeter and XBT measurements could give indication of their existence. Perhaps the most striking example of Rossby wave observations with T/P altimeter data is provided by Chelton and Schlax (1996), but several other analyses of the same nature have been carried out (e.g., Polito and Cornillon, 1997; Maltrud et al., 1998; White et al., 1998; Döös, 1999; Vivier et al., 1999; Witter and Gordon, 1999; Cipollini, 2000; Kobashi and Kawamura, 2001).

5. ALTIMETER DATA AND OCEANIC WIND-DRIVEN MODELS

A more advanced and promising application of altimeter-derived geostrophic currents is their analysis in the framework of oceanic models, in which currents are derived from the atmospheric forcing by solving appropriate dynamical equations. The comparison between *measured* and *modelled* currents allows to validate both the measuring technique and the model; moreover, discrepancies found from the comparison can reveal inadequacies both in the experimental and in the modelling approach, and can suggest possible improvements. The models can span from simple, classical wind-driven models such as the Sverdrup balance (see below) to extremely sophisticated state-of-the-art oceanic general circulation models (OGCMs) forced, for example, by ECMWF or NCEP surface fluxes. OGCMs allow for a detailed comparison with altimeter-derived currents (e.g., Chao and Fu, 1995; Stammer et al., 1996; Stammer, 1997; Fukumori et al., 1998), but it is sometimes difficult to identify physical mechanisms and interpret discrepancies, if all possible effects are taken into account. On the other hand, simplified models can sometimes allow for a better physical interpretation of the results, but they do not take into account effects that may interact with the ones considered. The use of both simple and sophisticated models appears to be the best way to proceed, as it is often done in recent studies.

Let us consider the Sverdrup balance as a prototype of simple but extremely interesting oceanic wind-driven model. The direct effect of the surface winds on the ocean is the transfer of horizontal momentum in the form of surface Ekman currents confined in a thin upper layer of frictional influence (the upper Ekman layer), in which the total transport is normal to the wind direction. The curl of the wind stress induces a divergence of the Ekman transport: the result is a displacement of the sea surface, with consequent generation of depth-independent geostrophic currents, that can be accompanied (as discussed in the preceding section) by depth-dependent relative currents. This is, in brief, the basic mechanism through which winds generate geostrophic currents in the ocean, and any theory aimed at explaining the general wind-driven circulation, and in particular the structure of the subtropical gyres (with a narrow and intense *western boundary current* and a broad and weak equatorward return flow in the oceanic interior) must be based on it. The model proposed by Sverdrup (1947) was the first to provide a relatively satisfactory explanation of the flow in the oceanic interior (i.e., away from the western boundary), and can be represented in terms of a stationary balance between the negative rate of change of planetary vorticity for the equatorward moving water columns and the negative vorticity input provided by the anticyclonic wind system, giving rise to the meridional Sverdrup mass transport (e.g., Pond and Pickard, 1983; Pedlosky, 1996):

$$M_y = \rho v H = \frac{curl_z \boldsymbol{\tau}}{\beta}, \tag{9}$$

where ρ is the water density, β is the derivative of *f* with respect to latitude, *y* is the meridional coordinate, *v* is the vertically averaged meridional component of the velocity (including Ekman and geostrophic currents), *H* is the water depth, and $\boldsymbol{\tau}$ is the surface wind stress. It is important to notice that the local balance (9) does not depend on neither the density structure nor the vertical distribution of velocity.

The possibility of using (9) (with $\boldsymbol{\tau}$ given by meteorological analysis) for a comparison with the meridional transport fluctuations computed from altimeter data by means of (7-8), relies on several assumptions, the main ones being: (a) the Ekman transport should be small compared to the geostrophic transport (or, alternatively, the Ekman transport should be subtracted from (9)); (b) topographic effects in the potential vorticity balance should be negligible (or, alternatively, they should be taken into account in the so-called *topographic Sverdrup balance*); (c) SSH fluctuations associated to baroclinic motions should be negligible; (d) the stationary relation (9) should also apply to time-dependent currents (time-dependent Sverdrup balance, TDSB).

Such a comparison has been carried out in recent studies (Fu and Davidson, 1995; Stammer, 1997; Isoguchi et al., 1997; Vivier et al., 1999). Interesting information are obtained for horizontally averaged transports: for instance, a significant indication of the TDSB in the high latitude North Pacific is obtained (Fu and Davidson, 1995; Stammer, 1997). At low latitudes things are quite different, as assumption (c) fails to hold. In a zonal belt centered at 13°N in the Pacific Ocean, Stammer (1997) found that the zonally averaged meridional Sverdrup transport anomaly, Q_{SVE}, and the corresponding anomaly obtained from T/P altimeter data under the assumption of barotropic flow, Q_{ALT}, are highly correlated signals with an important seasonal component. However, Q_{SVE} leads Q_{ALT} with a phase lag of about 3 months, moreover the Q_{ALT} rms is about an order of magnitude larger than the Q_{SVE} rms. Pierini (2002a) has proposed a dynamical interpretation of this result. A 2-layer primitive equation ocean model with free surface was implemented in an idealized Pacific ocean and was forced with a synthetic wind field (based on COADS and ECMWF wind data) representing a fairly realistic seasonal variability. The zonally integrated Sverdrup and altimeter-equivalent meridional transport anomalies obtained from the wind and the numerical free surface signal, respectively, yield phase shifts and relative amplitudes in good agreement with the above mentioned altimeter observations. A theoretical interpretation of these results is provided in terms of beta-refracted low latitude baroclinic Rossby waves generated at the eastern boundary. It should be noted, however, that such large difference between Q_{SVE} and Q_{ALT} does not imply that the TDSB does not hold in the tropics, but simply that the SSH anomaly cannot locally be used in (7-8) to compute vertically integrated transports, because assumption (c) does not hold. In fact, in the same study it was shown that the TDSB does hold in the framework of the numerical model, as Q_{SVE} models correctly the vertically integrated meridional transport anomaly computed from the numerical solution.

In general, even when agreement between Sverdrup and altimeter-derived meridional transport fluctuations is good for the seasonal signal, it must not be necessarily so for higher frequencies (corresponding to periods of up to few months); in other terms the failure of assumption (d) mentioned above should be considered. In fact, it is usually assumed that for periods above 1 month the Sverdrup balance is valid for time-dependent wind forcing (Willebrand et al., 1980), whereas it was recently shown (Pierini, 1997; 1998) that for periods $1<T<4$ months the oceanic response is in terms of westward intensified forced barotropic Rossby waves. This implies large departures from the TDSB over extensive western and central regions of the oceans. In a systematic analysis of the validity of the TDSB, in connection with altimeter data, Pierini (2002b) has found confirmation of this behaviour. Experimental evidence of westward confined barotropic Rossby waves based on T/P observations is provided, for example, by Kobashi and Kawamura (2001). In the same study by Pierini (2002b), topographic effects (related to the failure of assumption (b)) and effects associated to nonlinearities and to the complexity of the spatial structure of the wind stress curl have been considered as well. Finally, it should be pointed out that a very specific and advanced problem such as the assimilation of altimeter data into OGCMs has not been considered in this note.

5.1 Acknowledgments:

This work was supported by the "*Agenzia Spaziale Italiana*".

6. REFERENCES

Andersen, O.B., 1995: Global ocean tides from ERS 1 and TOPEX/POSEIDON altimetry. *J. Geophys. Res.*, **100**, 25,249-25,259.

Andersen, O.B., 1999: Shallow water tides in the northwest European shelf region from TOPEX/POSEIDON altimetry. *J. Geophys. Res.*, **104**, 7729-7741.

Andersen, O.B., P.L. Woodworth, and R.A. Flather, 1995: Intercomparison of recent ocean tide models. *J. Geophys. Res.*, **100**, 25,261-25,282.

Anderson, D.L.T., and A.E. Gill, 1975: Spin-up of a stratified ocean, with application to upwelling. *Deep-Sea Res.*, **22**, 583-596.

Arnault, S., and C. Le Provost, 1997: Regional identification in the Tropical Atlantic Ocean of residual tide errors from an empirical orthogonal function analysis of TOPEX/POSEIDON altimetric data. *J. Geophys. Res*., **102**, 21,011-21,036.

Buongiorno Nardelli, B., R. Santoleri, D. Iudicone, S. Zoffoli, and S. Marullo, 1999: Altimetric signal and three-dimensional structure of the sea in the Channel of Sicily. *J. Geophys. Res.*, **104**, 20,585-20,603.

Candela, J., 1991: The Gibraltar Strait and its role in the dynamics of the Mediterranean Sea. *Dyn. Atmos. Oceans*, **15**, 267-299.

Cartwright, D.E., and R.D. Ray, 1990: Oceanic tides from Geosat altimetry. *J. Geophys. Res*., **95**, 3069-3090.

Chambers, D.P., B.D. Tapley, and R.H. Stewart, 1998: Measuring heat storage changes in the equatorial Pacific: a comparison between TOPEX altimetry and Tropical Atmosphere-Ocean buoys. *J. Geophys. Res.*, **103**, 18,591-18,597.

Chao, Y., and L.L. Fu, 1995: A comparison between the TOPEX/POSEIDON data and a global ocean general circulation model during 1992-1993. *J. Geophys. Res*., **100**, 24,965-24,976.

Chelton, D.B., and M.G. Schlax, 1996: Global observations of oceanic Rossby waves. *Science*, **272**, 234-238.

Cipollini, P., D. Cromwell, G.D. Quartly, and P.G. Challenor, 2000: Remote sensing of oceanic extra-tropical Rossby waves. In "*Satellites, Oceanography and Society*", D. Alpern Editor, Elsevier Science, 99-123.

Desai, S.D., and J. M. Wahr, 1995: Empirical ocean tide models estimated from TOPEX/POSEIDON altimetry. *J. Geophys. Res*., **100**, 25,205-25,228.

Desai, S.D., J.M. Wahr, and Y. Chao, 1997: Error analysis of empirical ocean tide models estimated from TOPEX/POSEIDON altimetry. *J. Geophys. Res.*, **102**, 25,157-25,172.

Döös, K., 1999: Influence of the Rossby waves on the seasonal cycle in the Tropical Atlantic. *J. Geophys. Res*., **104**, 29,591-29,598.

Eanes, R.J., and S.V. Bettadpur, 1995: The CSR3.0 Global Ocean Tide Model. *Publ. CSR-TM-95-06*, Center for Space Res. , Univ. of Texas at Austin.

Feron, R.C.V., W.P.M. De Ruijter, and P.J. Van Leeuwen, 1998: A new method to determine the mean sea surface dynamic topography from satellite altimeter observations. *J. Geophys. Res.*, **103**, 1343-1362.

Foreman, M.G.G., W.R. Crawford, J.Y. Cherniawsky, J.F.R. Gower, L. Cuypers, and V.A. Ballantyne, 1998: Tidal correction of TOPEX/POSEIDON altimetry for seasonal sea surface elevation and current determination off the Pacific coast of Canada. *J. Geophys. Res*., **103**, 27,979-27,998.

Fu, L.L., E.J. Christensen, C.A. Yamarone, Jr., M. Lefebvre, Y. Ménard, M. Dorrer, and P. Escudier, 1994: TOPEX/POSEIDON mission overview. *J. Geophys. Res*., **99**, 24,369-24,381.

Fu, L.L., and R.A. Davidson, 1995: A note on the barotropic response of sea level to time-dependent wind forcing. *J. Geophys. Res*., **100**, 24,955-24,963.

Fu, L.L., and G. Pihos, 1994: Determining the response of sea level to atmospheric pressure forcing using TOPEX/POSEIDON data. *J. Geophys. Res.*, **99**, 24,633-24,642.

Fukumori, I., Raghunath, R., and L.L. Fu, 1998: Nature of global large-scale sea level variability in relation to atmospheric forcing: A modeling study. *J. Geophys. Res*., **103**, 5493-5512.

Gaspar, P., and R.M. Ponte, 1997: Relation between sea level and barometric pressure determined from altimeter data and model simulations. *J. Geophys. Res*., **102**, 961-971.

Gill, A.E., 1982: *Atmosphere-Ocean Dynamics*. Academic Press, 662 pp.

Gill, A.E., and P.P. Niiler, 1973: The theory of the seasonal variability in the ocean. *Deep Sea Res*., **20**, 141-177.

Gilson, J., D. Roemmich, B. Cornuelle, and L.L. Fu, 1998: Relationship of TOPEX/POSEIDON altimetric height to steric height and circulation in the North Pacific. *J. Geophys. Res*., **103**, 27,947-27,965.

Han, G., and C.L. Tang, 1999: Velocity and transport of the Labrador Current determined from altimetric, hydrographic, and wind data. *J. Geophys. Res*., **104**, 18,047-18,057.

Holton, 1979: *An Introduction to Dynamic Meteorology*. Academic Press.

Isoguchi, O., H. Kawamura, and T. Kono, 1997: A study on wind-driven circulation in the subarctic North Pacific using TOPEX/POSEIDON altimeter data. *J. Geophys. Res*., **102**, 12,457-12,468.

Iudicone, D., R. Santoleri, S. Marullo, and P. Gerosa, 1998: Sea level variability and surface eddy statistics in the Mediterranean Sea from TOPEX/POSEIDON data. *J. Geophys. Res.*, **103**, 2995-3011.

Kantha, L.H., 1995: Barotropic tides in the global oceans from a nonlinear tidal model assimilating altimetric tides. 1. Model description and results. *J. Geophys. Res*., **100**, 25,283-25,308

Kantha, L.H., C. Tierney, J.W. Lopez, S.D. Desai, M.E. Parke, and L. Drexler, 1995: Barotropic tides in the global oceans from a nonlinear tidal model assimilating altimetric tides. 2. Altimetric and geophysical implications. *J. Geophys. Res.*, **100**, 25,309-25,317.

Kelly, K.A., and S.T. Gille, 1990: Gulf Stream surface transport and statistics at 69°W from the Geosat altimeter. *J. Geophys. Res.*, **95**, 3149-3161.

Kobashi, F., and H. Kawamura, 2001: Variation of sea surface height at periods of 65-220 days in the subtropical gyre of the North Pacific. *J. Geophys. Res.*, **106**, 26,817-26,831.

Larnicol, G., P.Y. Le Traon, N. Ayoub, and P. De Mey, 1995: Mean sea level and surface circulation variability of the Mediterranean Sea from 2 years of TOPEX/POSEIDON altimetry. *J. Geophys. Res*., **100**, 25,163-25,177.

Le Provost, C., M.L. Genco, F. Lyard, P. Vincent, and P. Canceil, 1994: Spectroscopy of the world ocean tides from a hydrodynamic finite element model. *J. Geophys. Res.*, **99**, 24,777-24,797.

Le Traon, P.Y., and P. Gauzelin, 1997: Response of the Mediterranean, mean sea level to atmospheric pressure forcing. *J. Geophys. Res*., **102**, 973-984.

Ma, X.C., C.K. Schum, R.J. Eanes, and B.D. Tapley, 1994: Determination of ocean tides from the first year of TOPEX/POSEIDON altimeter measurements. *J. Geophys. Res.*, **99**, 24,809-24,820.

Maltrud, M.E., R.D. Smith, A.J. Semtner, and R.C. Malone, 1998: Global eddy-resolving ocean simulations driven by 1985-1995 atmospheric winds. *J. Geophys. Res.*, **103**, 30,825-30,853.

Matsumoto, K., M. Ooe, T. Sato, and J. Segawa, 1995: Ocean tide model obtained from TOPEX/POSEIDON altimetry data. *J. Geophys. Res*., **100**, 25,319-25-330.

Munk, W.H., and D.E. Cartwright, 1966: Tidal spectroscopy and prediction. *Philos. Trans. R. Soc. London*, A, **259**, 533-583.

Nerem, R.S., et al., 1994: Gravity model development for TOPEX/Poseidon: Joint gravity model 1 and 2. *J. Geophys. Res*., **99**, 24,405-24,448.

Park, Y.H., and L. Gambéroni, 1995: Large-scale circulation and its variability in the south Indian Ocean from TOPEX/POSEIDON altimetry. *J. Geophys. Res*., **100**, 24,911-24,929.

Pedlosky, J., 1987: *Geophysical Fluid Dynamics*. Springer-Verlag, 710 pp.

Pedlosky, J. 1996: *Ocean Circulation Theory*. Springer-Verlag, 453 pp.

Pickard, G.L., and W.J. Emery, 1982: *Descriptive Physical Oceanography*. Pergamon Press, 249 pp.

Pierini, S., 1996: Topographic Rossby modes in the Strait of Sicily. *J. Geophys. Res*., **101**, 6429-6440.

Pierini, S., 1997: Westward intensified and topographically modified planetary modes. *J. Phys. Oceanogr*., **27**, 1459-1471.

Pierini, S., 1998: Wind-driven fluctuating western boundary currents. *J. Phys. Oceanogr*., **28**, 2185-2198.

Pierini, S., 2002a: A model for the dynamical interpretation of the altimeter-derived seasonal variability in the North Pacific Ocean. Submitted.

Pierini, S., 2002b: An analysis of the validity of the time-dependent Sverdrup balance, with application to altimeter data. In preparation.

Pierini, S., A. Fincham, D. Renouard, R. D'Ambrosio, and H. Didelle, 2002: Laboratory modeling of topographic Rossby normal modes. *Dyn. Atmos. Oceans*, in press.

Polito, P.S., and P. Cornillon, 1997: Long baroclinic Rossby waves detected by TOPEX/POSEIDON. *J. Geophys. Res*., **102**, 3215-3235.

Pond, S., and G.L. Pickard, 1983: *Introductory Dynamical Oceanography*. Pergamon Press, 329 pp.

Ponte, R.M., 1992: The sea level response of a stratified ocean to barometric pressure forcing. *J. Phys. Oceanogr*., **22**, 109-113.

Ponte, R.M., 1993: Variability in a homogeneous global ocean forced by barometric pressure. *Dyn. Atmos. Oceans*, **18**, 209-234.

Ponte, R.M., 1997: Nonequilibrium response of the global ocean to the 5-day Rossby-Haurwitz wave in atmospheric surface pressure. *J. Phys. Oceanogr*., **27**, 2158-2168.

Ponte, R.M., and P. Gaspar, 1999: Regional analysis of the inverted barometer effect over the global ocean using TOPEX/POSEIDON data and model results. *J. Geophys. Res*., **104**, 15,587-15-601.

Rapp, R.H., Y.M. Ming, and N.K. Pavlis, 1991: The Ohio State 1991 geopotential and sea surface topography harmonic coefficient model. Rep. 410, Dep. of Geod. Sci. and Surve., Ohio State Univ..

Rapp, R.H., C. Zhang, and Y. Yi, 1996: Analysis of dynamic ocean topography using TOPEX data and orthonormal functions. *J. Geophys. Res*., **101**, 22,583-22,598.

Robinson, I.S., 1994: *Satellite Oceanography*. Wiley, 455 pp.

Sanchez, B.V., and N.K. Pavlis, 1995: Estimation of main tidal constituents from TOPEX altimetry using a Proudman function expansion. *J. Geophys. Res*., **100**, 25,229-25-248.

Schlax, M.G., and D.B. Chelton, 1994: Aliased tidal errors in TOPEX/POSEIDON sea surface height data. *J. Geophys. Res*., **99**, 24,761-24,776.

Semtner, A.J., Jr., and R.M. Chervin, 1992: Ocean general circulation from a global eddy-resolving model. *J. Geophys. Res.*, **97**, 5493-5550.

Shum, C.K., et al., 1997: Accuracy assessment of recent ocean tide models. *J. Geophys. Res*., **102**, 25,173-25,194.

Snaith, H.M., and I.S. Robinson, 1996: A study of currents south of Africa using Geosat satellite altimetry. *J. Geophys. Res*., **101**, 18,141-18,154.

Stammer, D., 1997: Steric and wind-induced changes in TOPEX/POSEIDON large-scale sea surface topography observations. *J. Geophys. Res*., **102**, 20,987-21,009.

Stammer, D., R. Tomakian, A. Semtner, and C. Wunsch, 1996: How well does a 1/4° global circulation model simulate large-scale oceanic observations? *J. Geophys. Res*., **101**, 25,779-25,881.

Strub, P.T., T.K. Chereskin, P.P. Niiler, C. James, and M.D. Levine, 1997: Altimeter-derived variability of surface velocities in the California Current System. 1. Evaluation of TOPEX altimeter velocity resolution. *J. Geophys. Res.*, **102**, 12,727-12,748.

Sverdrup, H.U., 1947: Wind-driven currents in a baroclinic ocean, with application to the equatorial currents of the eastern Pacific. *Proc. Natl. Acad. Sci. USA*, **33**, 318-326.

Tapley, B.D., et al., 1996: The JGM-3 gravity model. *J. Geophys. Res*., **101**, 28,029-28,049.

Tierney, C.C., M.E. Parke, and G.H. Born, 1998: An investigation of ocean tides derived from along-track altimetry. *J. Geophys. Res*., **103**, 10,273-10,287.

Vivier, F., K.A. Kelly, and L.A.Thompson, 1999: Contributions of wind forcing, waves, and surface heating to sea surface height observations in the Pacific Ocean. *J. Geophys. Res.*, **104**, 20,767-20,788.

Vivier, F., and C. Provost, 1999: Volume transport of the Malvinas current: can the flow be monitored by TOPEX/POSEIDON? *J. Geophys. Res*., **104**, 21,105-21,122.

White, W.B., Y. Chao, and C.K. Tai, 1998: Coupling of biennial oceanic Rossby waves with the overlying atmosphere in the Pacific basin. *J. Phys. Oceanogr*., **28**, 1236-1251.

White, W.B., and C.K. Tai, 1995: Inferring interannual changes in global upper ocean heat storage from TOPEX altimetry. *J. Geophys. Res*., **100**, 24,943-24,954.

Willebrand, J., S.G.H. Philander, and R.C. Pakanowski, 1980: The oceanic response to large-scale atmospheric disturbances. *J. Phys. Oceanogr*., **10**, 411-429.

Williams, R.G., and M. Pennington, 1999: Combining altimetry with a thermocline model to examine the transport of the North Atlantic. *J. Geophys. Res.*, **104**, 18,269-18,280.

Witter, D.L., and A.L. Gordon, 1999: Interannual variability of South Atlantic circulation from 4 years of TOPEX/POSEIDON satellite altimeter observations. *J. Geophys. Res*., **104**, 20,927-20,948.

Wunsch, C., and D. Stammer, 1995: The global frequency-wavenumber spectrum of oceanic variability estimated from TOPEX/POSEIDON altimetric measurements. *J. Geophys. Res*., **100**, 24,895-24,910.

Wunsch, C., and D. Stammer, 1997: Atmospheric loading and the oceanic “inverted barometer” effect. *Rev. Geophys*., **35**, 79-107.

Yu, Y., W.J. Emery, and R.R. Leben, 1995: Satellite altimeter derived geostrophic currents in the western tropical Pacific during 1992-1993 and their validation with drifting buoy trajectories. *J. Geophys. Res.*, **100**, 25,069-25,085.